Supporting Information

First-Principles Unraveling of Structure-Catalytic Activity Nexus and Mechanistic of δ-MnO_2-Supported Metal Cluster Catalystst in Ambient Temperature Benzene to CO_2 Degradation

Jiangmei Yan[a], Peng Zhang[a], Dan Chen[a], Jie Cheng[a], Mengshan Song[b], Shuai Li[b], Hui Zhao[b], Guo Chang[b], Yuefeng Li[a], Lihui Zeng[a], Ruqian Lian[c], Chuangwei Liu*[d], Wangtu Huo*[b], Dongxiao Kan*[b]

[a]Kaili Catalyst & New Materials Co., Ltd, Xi' an, 710201, China

[b]Northwest Institute for Non-ferrous Metal Research, Xi' an, 710016, China

[c]Hebei Research Center of the Basic Discipline for Computational Physics College of Physics Science and Technology, Hebei University, Baoding 071002, P. R. China

[d]Dalian Institute of Chemical Physics, Chinese Academy of Sciences, Dalian, 116023 China

*Corresponding Author: dxkan1202@126.com; cwliu@dicp.ac.cn; rqlian@126.com; huowangtu_1988@163.com

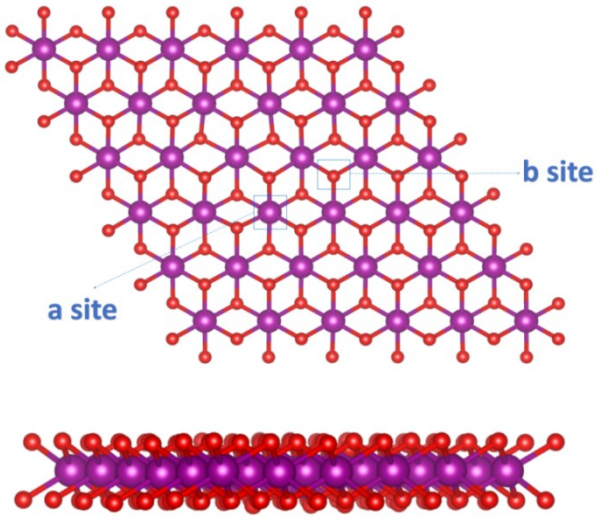

Figure S1 Two distinct positions of single metal loading on the δ-MnO_2(001) surface, designated as "a site" and "b site".

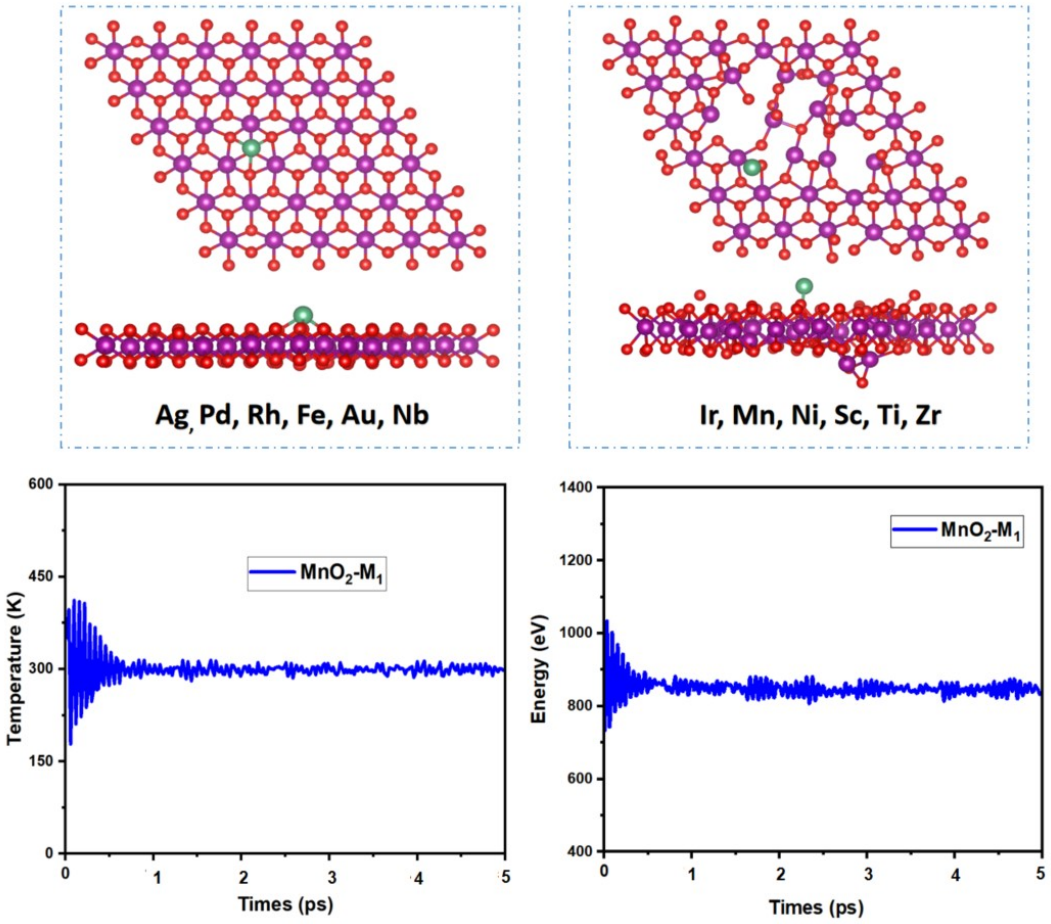

Figure S2 Thermodynamic stabilities of the 12 single-atom catalysts (SACs) at 300 K following 5 ps of molecular dynamics simulation.

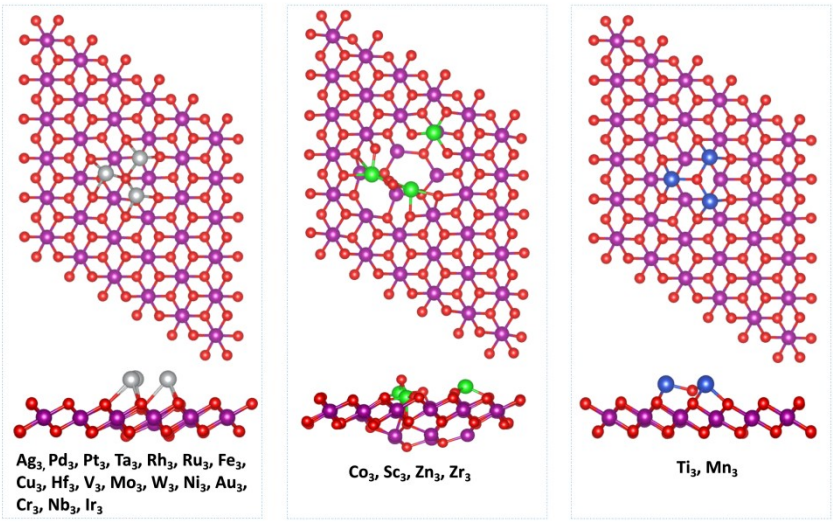

Figure S3 Structural stabilities of the 23 types of trimers after optimization.

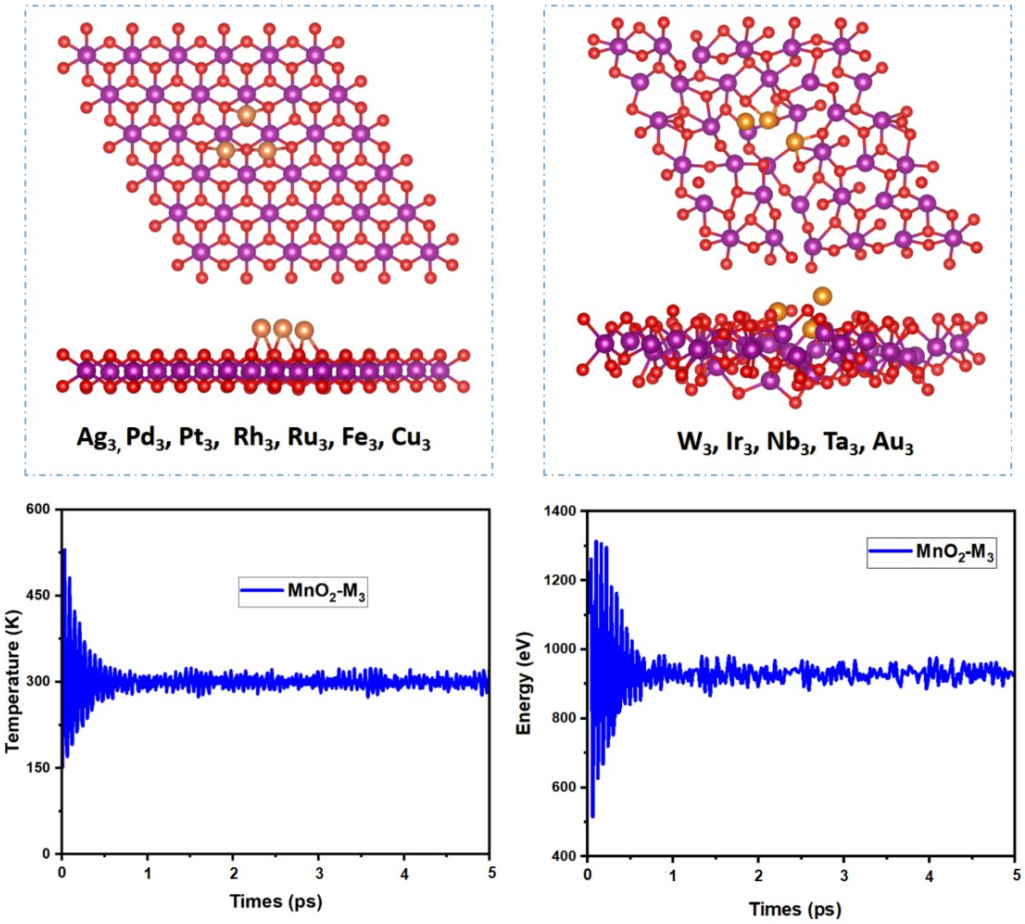

Figure S4 Energy-time curve and structures obtained from molecular dynamics simulations at room temperature over a duration of 5 ps.

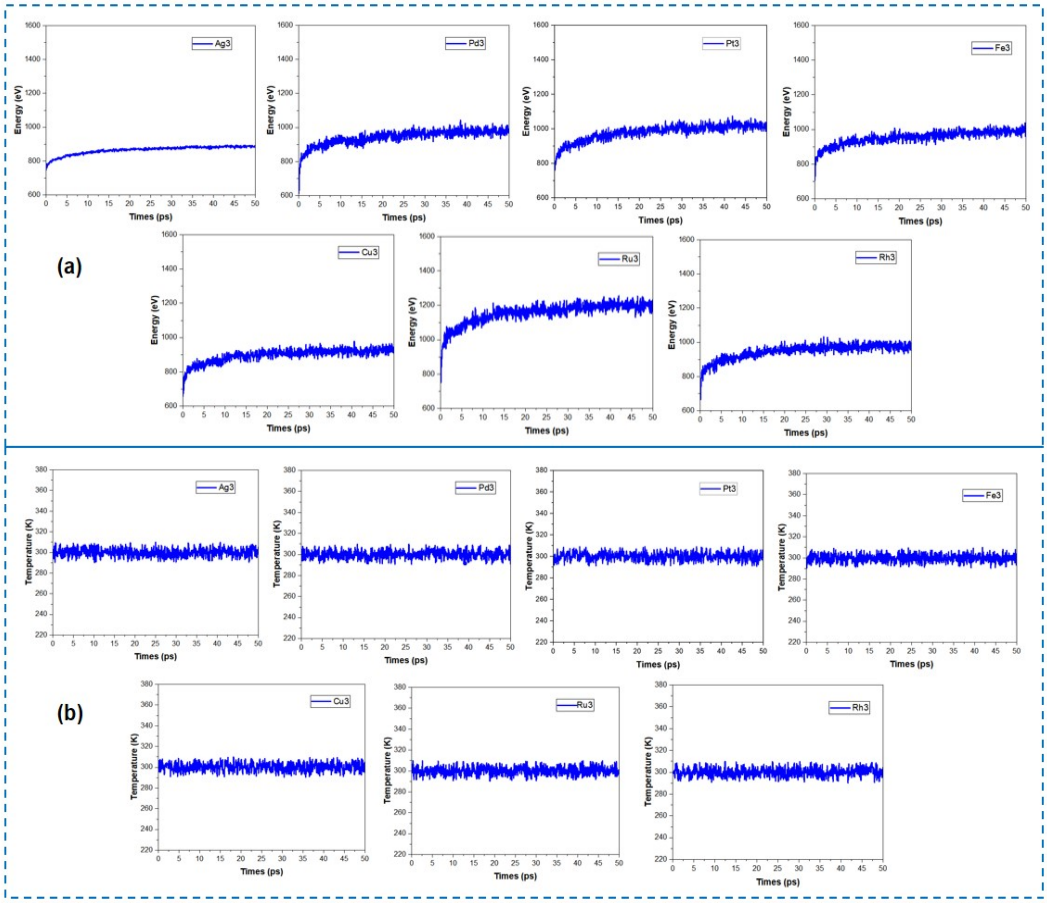

Figure S5 Energy-time curve and structures obtained from molecular dynamics simulations for δ-MnO_2-M_3 at room temperature over a duration of 50 ps.

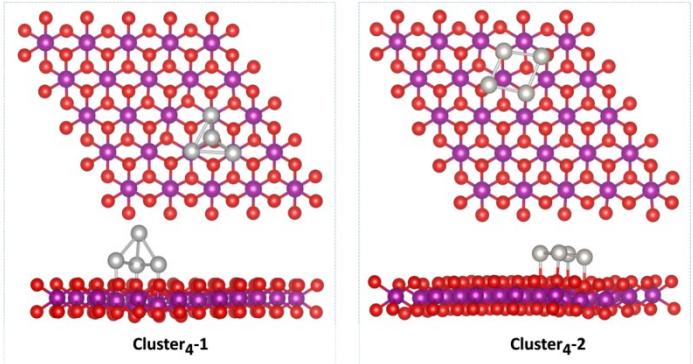

Figure S6 Two possible configurations of tetramers: cluster$_4$-1, which is a tetrahedron, and cluster$_4$-2, which is a parallelogram model..

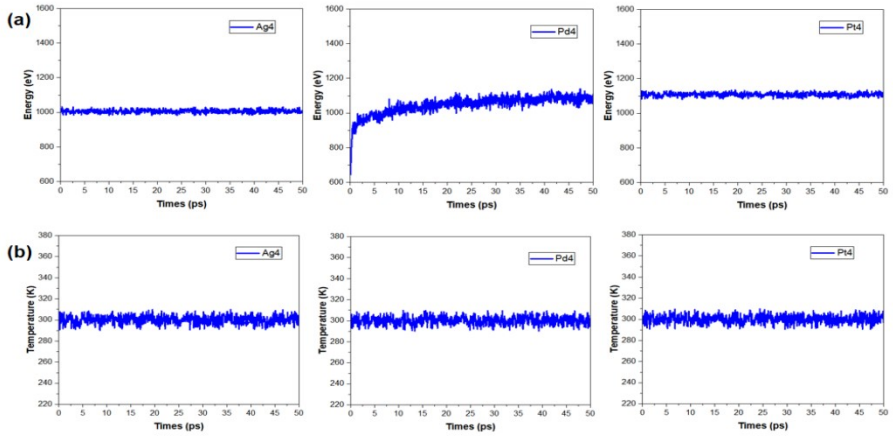

Figure S7 Energy-time curve and structures obtained from molecular dynamics simulations for δ-MnO_2-M_4 at room temperature over a duration of 50 ps.

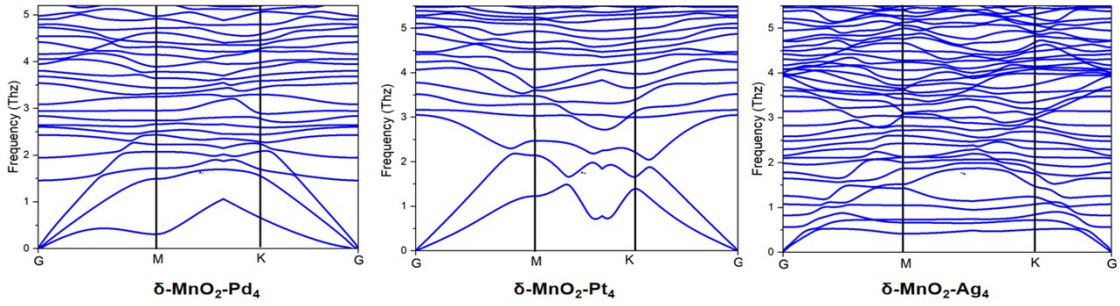

Figure S8 The phonon spectrum of δ-MnO_2-Ag_4, δ-MnO_2-Pd_4, and δ-MnO_2-Pt_4

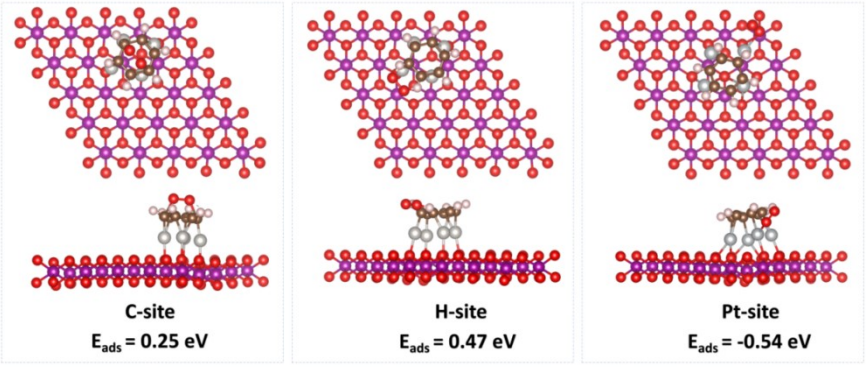

Figure S9 Adsorption energies and structures of O_2 molecule on the three possible sites of the benzene-adsorbed models.

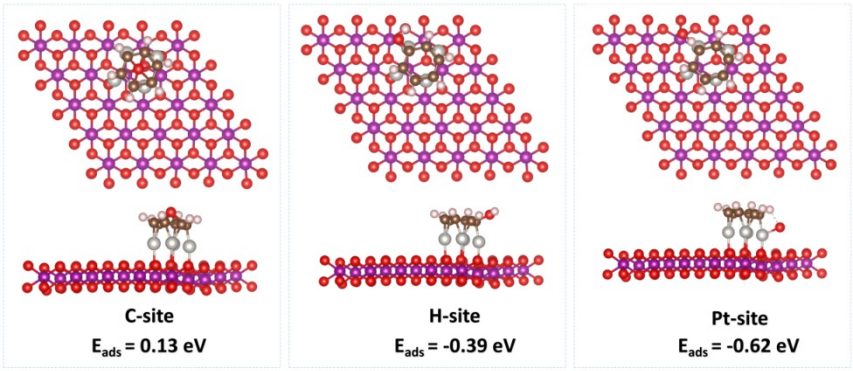

Figure S10 Adsorption energies and structures of O atom on the three possible sites of the benzene-adsorbed models.

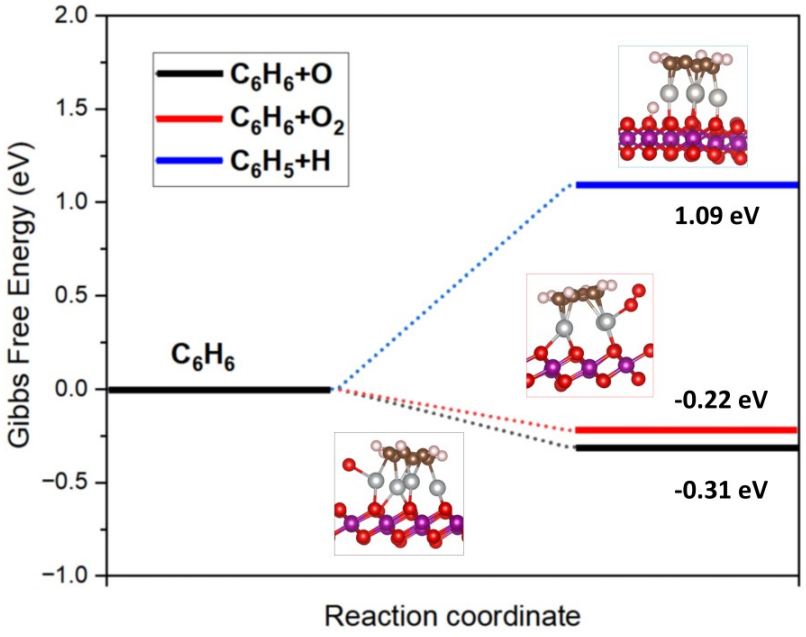

Figure S11 Gibbs free energies of the first step in benzene degradation, including the adsorbed benzene combined with O atom, combined with O_2 molecule, or dehydrogenation, respectively.

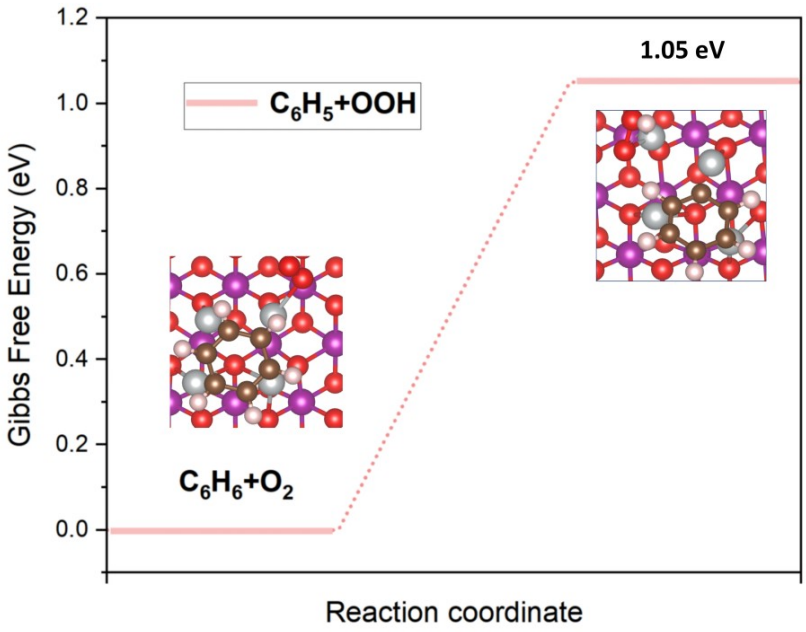

Figure S12 Gibbs free energies of the adsorbed O_2 molecule abstracting an H from the adsorbed benzene and generating a pair of C_6H_5 and OOH molecules.

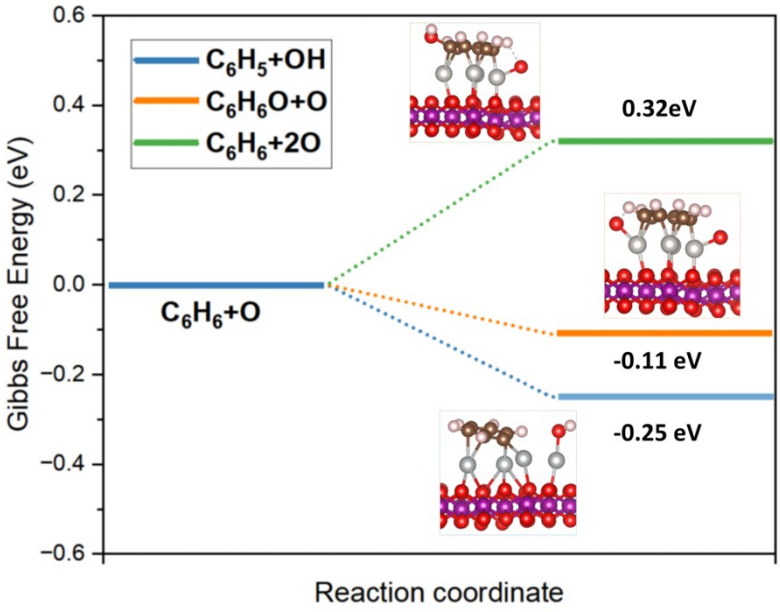

Figure S13 Gibbs free energies of the second step in benzene degradation via the O atom combination path, including benzene dehydrogenated to form C_6H_5 + OH, and further oxygenation (addition of O_1) to form C_6H_6 + 2O and C_6H_6O + O, respectively.

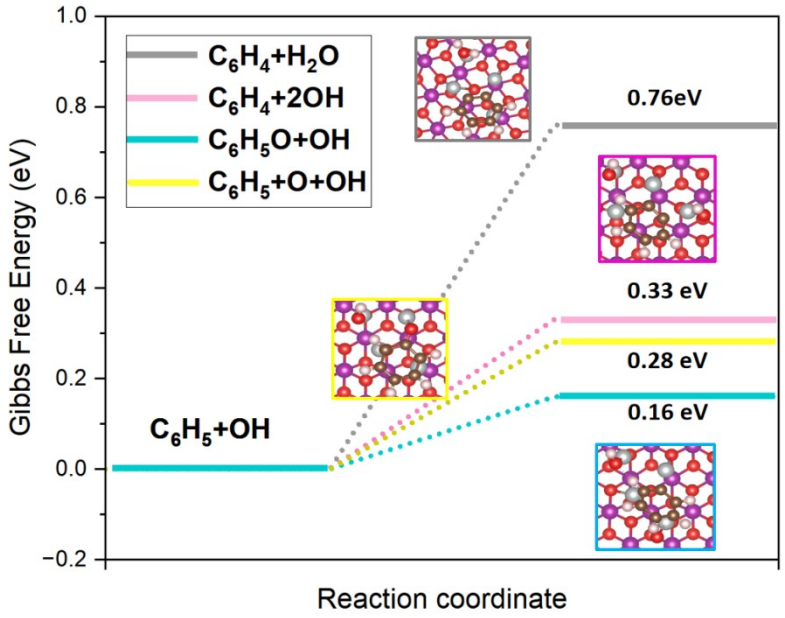

Figure S14 Gibbs free energies of the third step in benzene degradation via the O atom combination path, which consists of four possible routes: further oxygenation (addition of O_2) to form C_6H_6O + OH, C_6H_5 + OH + O, or C_6H_4 + 2OH, or dehydrogenation to form C_6H_4 + H_2O

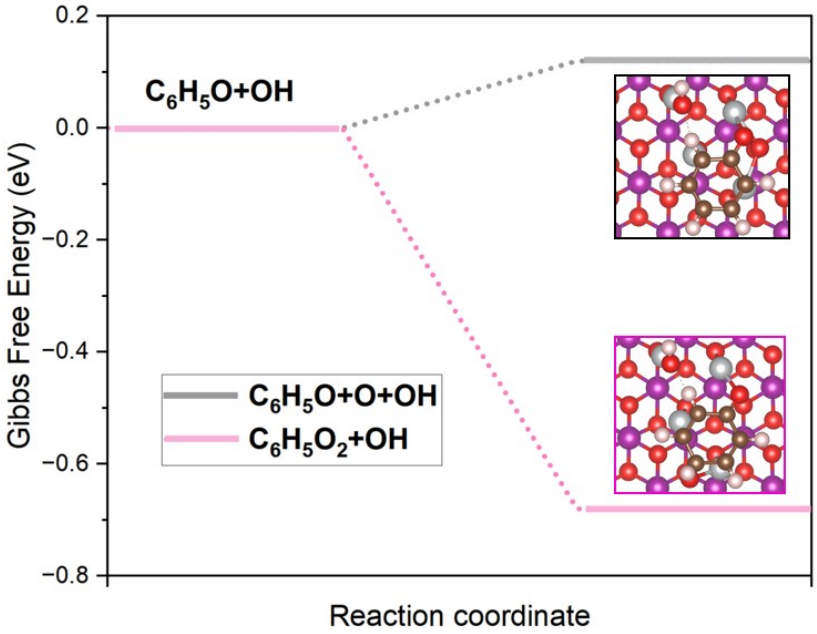

Figure S15 Gibbs free energies of the fourth step in benzene degradation via the O atom combination path, which exhibits two courses: the third O (O_3) binding to Pt and generating C_6H_5O + O + OH, or connecting with benzene to form $C_6H_5O_2$ + OH.

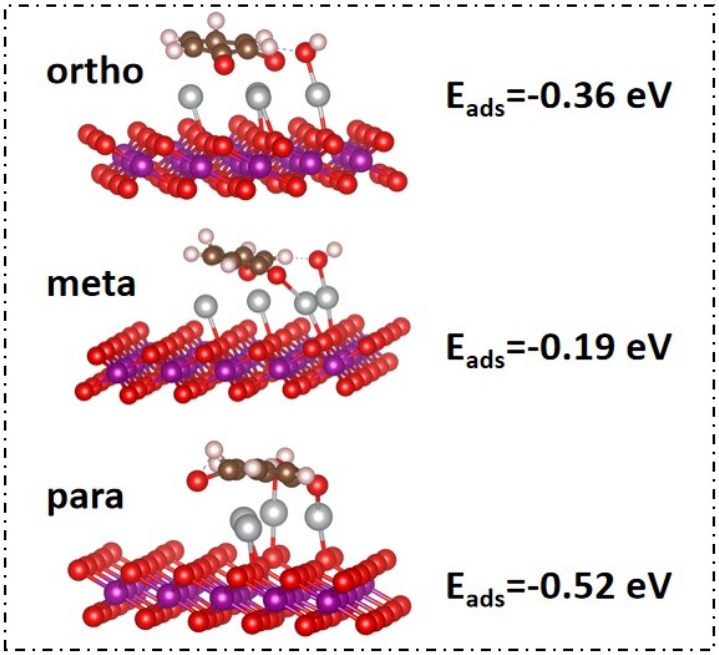

Figure S16 Three possible sites (namely ortho, meta, and para sites) and corresponding adsorption energies of the O_3 attached to the adsorbed C_6H_5O molecule.

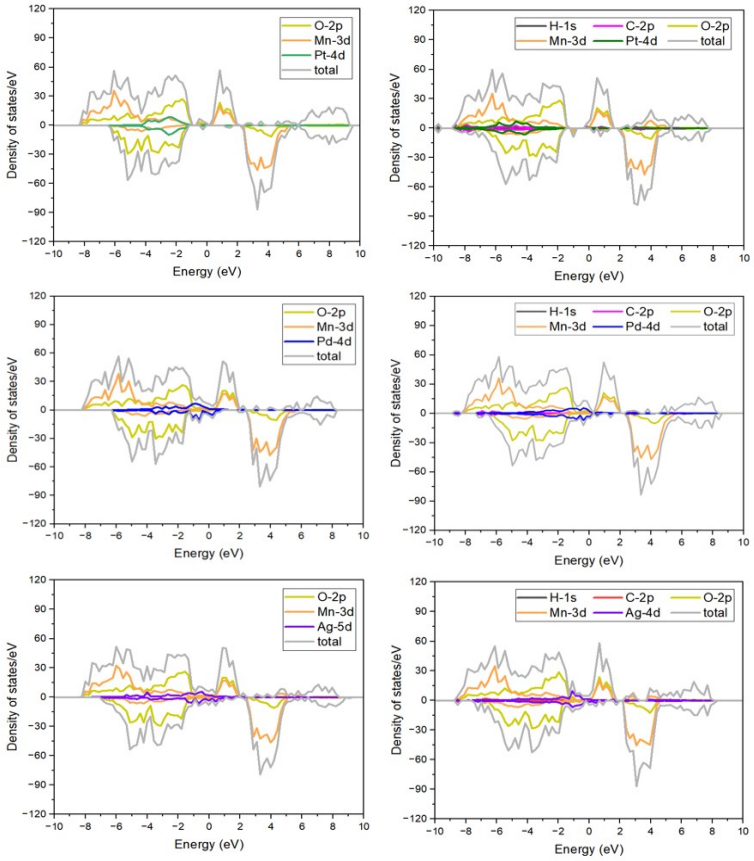

Figure S17 The projected density of states for δ-MnO_2-Ag_4, δ-MnO_2-Pd_4, and δ-MnO_2-Pt_4 before and after benzene adsorption.

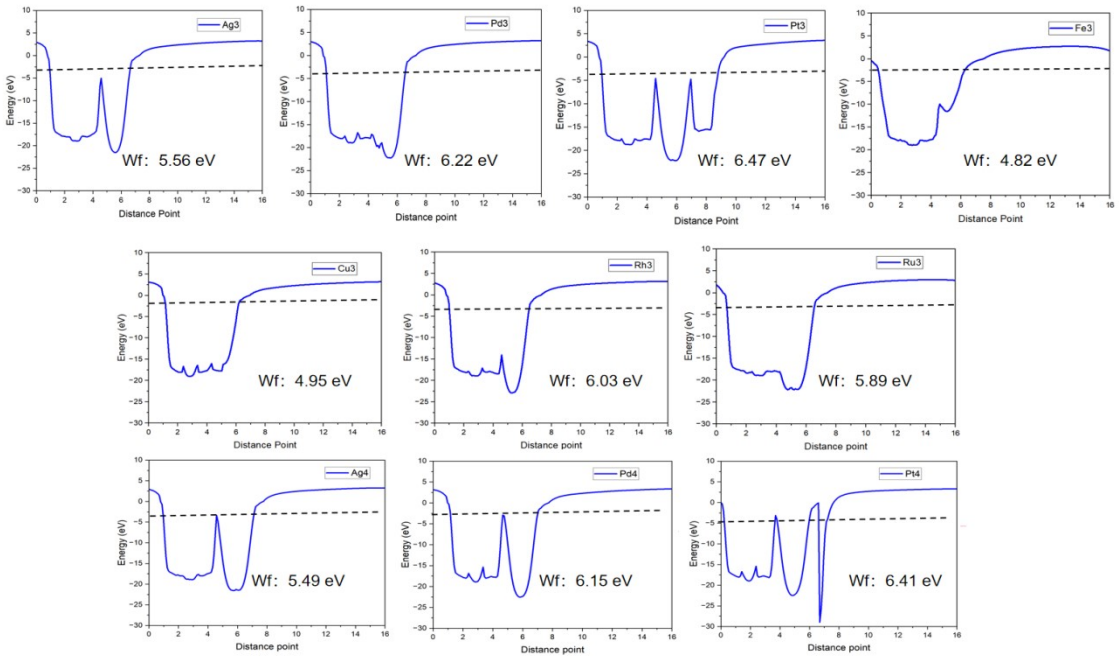

Figure S18 The calculated work function values of δ-MnO_2-M_3 (Ag_3, Pd_3, Pt_3, Cu_3, Fe_3, Rh_3, Ru_3) and δ-MnO_2-M_4 (Ag_4, Pd_4, Pt_4).

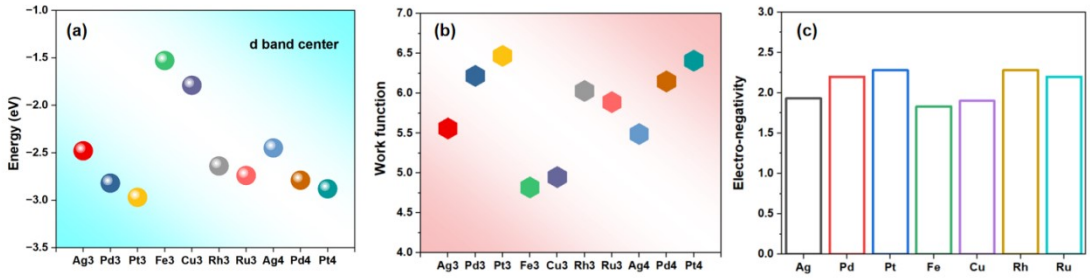

Figure S19 (a) The d band center and (b) work function values of δ-MnO_2-M_3 (Ag_3, Pd_3, Pt_3, Cu_3, Fe_3, Rh_3, Ru_3) and δ-MnO_2-M_4 (Ag_4, Pd_4, Pt_4); (c) the electronegativities of the referred metals (Ag, Pd, Pt, Cu, Fe, Rh, Ru).